Nanostructuring surfaces: Deconstruction of the Pt(110)-(1x2) surface by C60

Xavier Torrelles, Véronique Langlais, Maurizio de Santis, Hélio Tolentino, Yves Gauthier

Nanostructuring surfaces: deconstruction of Pt(110)-(1x2) surface by C60

X. Torrelles[1], V. Langlais[2,3], M. De Santis[3], H. Tolentino[3] & Y. Gauthier[3]
[1]*Institut de Ciencia de Materials de Barcelona, ICMAB-CSIC, 08193 Bellaterra, Barcelona (Spain)*
[2]*University Autonomous of Barcelona, UAB, 08193 Bellaterrra, Barcelona (Spain)*
[3]*Institut Néel, CNRS & Université Joseph Fourier, BP 166, F-38042 Grenoble (France)*
(Received on *date*; published on *date*)

When deposited on metal surfaces, C60 creates nanoholes. Grazing incidence X-rays diffraction reveals a c(4x4) reconstruction induced by C60 on Pt(110)-(1x2). While the initial (1x2) missing row is partially deconstructed, under each fullerene we find double atomic vacancy involving two Pt layers. The resulting interface is deeply modified with a 75% Pt occupancy and regularly distributed double vacancy. The orientation of the molecule is compatible with local surface *cm* symmetry with a pentagonal ring almost parallel to the surface while hexagonal rings are almost parallel to the (111) facets of the nanohole. The short nearest neighbor C60 distances increase the Van der Waals repulsion forces that are minimized by a charge transfer between molecule and substrate involving a large number of C-Pt bonds and a reduction of 6% of the apparent diameter of the C60 molecule.

DOI:

PACS number(s):

2D molecular ordering is often accompanied by surface restructuring of the 2-3 topmost atomic layers: such a modified interface may thus be used for both surface moulding and surface nanopatterning, with relevant technological applications[1-4]. The mechanism of molecule's surface anchoring is usually quite complex due to the interplay between intermolecular bonds and molecule-substrate interactions involving a large number of adsorption sites. This may result in either displacive substrate reconstructions, involving extensive mass transport, which can be accompanied by a structural deformation of the adsorbed molecules. Formation of vacancies has already been observed on Pt(111)[4], Pd(110)[5-6], Ag(110)[7], Ag[111][8], and Au(110)[9]. The shape and size of the nanoholes affect the actual properties of C60. To fully understand the molecular film properties, the molecule-substrate system has to be considered as a whole and the isolated molecules properties cannot be simply transferred to the monolayer case. Grazing incidence X-rays diffraction (GIXRD) allows not only determining the substrate structure and C60 orientation, but also the nature of the bonds formed between C60 and Pt.

The Pt(110)-(1x2) missing row surface was prepared by argon sputtering and annealing (T = 970 K) cycles, followed by cooling down to 850 K under oxygen partial pressure. The resulting (1x2) domains size was of typically 2000 Å as determined from the scan width of the (0, ½, 0.05) reflection. C60 (purity 99.9%) was sublimated, from an alumina crucible kept at 750 K, on the Pt sample maintained at ~810 K. The fullerene coverage was calibrated recording the C_{273}/Pt_{247} Auger peak-to-peak ratio. As previously reported[10], this experimental procedure results in a single adsorbed fullerene layer on the surface. The spectra were collected at BM32 beamline[11] of the European Synchrotron Radiation Facility, ESRF. The X-ray beam was generated by a bending magnet, monochromatised with a water-cooled double crystal Si(111) monochromator and sagitally focused. The energy and size at the sample of the incident beam were set to 18.0 keV and 0.5 mm x 0.1 mm (horizontal x vertical dimensions at the sample surface) with a constant incidence angle of 0.25º. The integrated intensities were recorded by rocking the crystal around its surface normal. A total of 1775 reflections, specific to the c(4x4) structure, were measured, which reduced to 1221 after averaging of the equivalent reflections[12] involving 45 Fractional Order Rods (FORs) and 9 Crystal Truncation Rods (CTRs). The Pt(110) surface is described by lattice vectors (a_1, a_2, a_3) parallel to the [1-10], [001], and [110] directions, respectively, where $a_1=a_3=a_0/\sqrt{2}$, $a_2=a_0$ (a_0= bulk lattice constant). H, K, L denote the coordinates of the corresponding reciprocal lattice vectors. The new lattice parameters corresponding to this

c(4x4) cell become $(a'_1,a'_2,a_3)=(4*a_1, 4*a_2, a_3)$. The standard deviations σ_{HKL} of the structure factors F_{HKL} were evaluated by the quadrature sum of a systematic error estimated close to 11% and statistical error[13]. From the analysis of the experimental data the *c2mm* plane group symmetry was determined. Calculations were performed with a modified version of ROD[14] used to optimize the agreement fit factor χ^2.

First of the all, the data analysis was performed without assumption taking into account that the substrate structure is a first order parameter, compared to the actual position and orientation of the molecule due to the atomic number difference. The initial calculations, using the CTRs and FORs, were based on the (1x2) reconstruction of the clean surface which fulfils the *c2mm* experimental symmetry. The atomic density of all sites in the three topmost layers was then let free to vary in order to find out which atomic positions were actually occupied by Pt atoms. This procedure was carried out to determine the shape and size of the nanoholes, if any, hosting the molecule and compatible with the measured symmetry. The final analysis included 48 independent Pt atoms distributed over 5 layers and one molecule. We determined a total of 62 positional coordinates for bulk atoms simultaneously with the height of the C60 and 3 Euler angles for its orientation. Seven isotropic thermal vibration parameters[15] were also optimized (one for the fullerenes, two for the topmost Pt layer and one for each of the 4 deeper Pt layers).

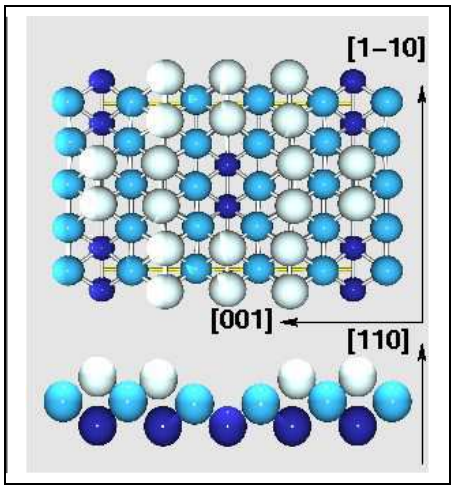

Fig. 1: (color online) Pt(110)-c(4x4): Top and lateral views of the optimum surface slab ordering showing the geometry and distribution of the nanoholes (two layers) on the Pt(110)-surface. Note the shift of some atoms perpendicular to the dense rows. Darker color atoms correspond with deeper surface atoms.

In figure 1 is depicted the substrate model respecting the experimental symmetry consisting of a Pt top layer with complete rows alternating with half filled ones yielding a 75% occupancy with double vacancies alternating with Pt doublets. The molecules were then considered in a second step, with C60 supposed to reside in the optimum substrate configuration (fig. 1) and compatible with a *c2mm* symmetry (configuration C2 of Fig.2). The c(4x4) unit cell contains one fullerene and an unique nanohole: as a consequence, in this dense quasi-hexagonal phase, all C60 have the same orientation and the same double vacancy adsorption site.

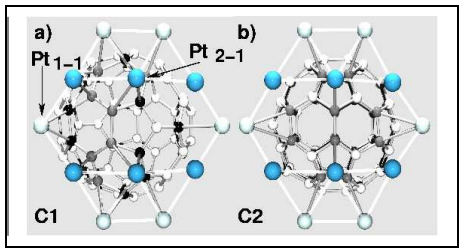

Fig. 2: (color online) Bottom view of C60 balls showing the C1 (a) and C2 (b) configurations bonded to the two topmost surface Pt-layers: the C60 molecule approximately places a 5 bond (pentagon almost parallel to the surface) or a 6:6 bond (hexagon:hexagon bond) on a bridge site of the second Pt layer, respectively. Black or gray atoms in C1 indicate C-atoms with shorter or larger C-Pt distances than 2.4 Å, respectively. Topmost or second surface Pt layers are indicated with light (whiter) or (darker) sky blue colors, respectively.

As the fit agreement with this C2 model was moderate ($\chi^2 \approx 2.1$) the surface symmetry was released to *cm,* with the mirror plane parallel to the [1-10] direction. The lowest χ^2-value ($\approx$ 1.5) was obtained with the C1-configuration model (Fig. 2a) and the presence of two mirrored domains to reproduce the experimental *c2mm* symmetry. In the final stage, C60 balls were allowed to rotate, around an axis parallel to [001] direction, and translate, parallel to [1-10] direction, with respect to the initial C2 adsorption configuration. The final configuration of the system is shown in Fig. 3 while Fig. 4 shows some representative data of the fit quality.

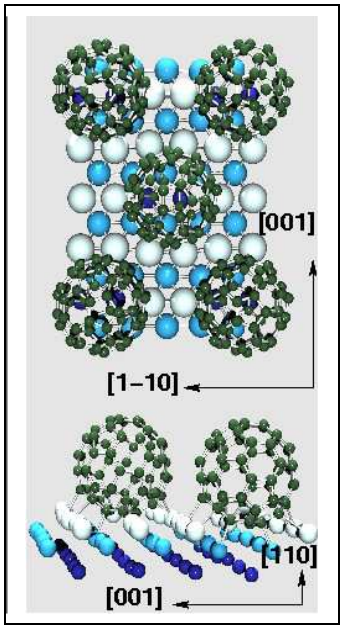

Fig. 3: Top and lateral views of the C60/Pt(110)-c(4x4) superstructure showing the best and most plausible orientation of the C60 molecules according to the least squares refinement procedure. The structure corresponds with a C60 molecule with a pentagon ring parallel to the substrate surface shifted 0.5 Å long [1-10] direction and located on Pt bridge sites.

The C60 molecules are located on the bi-atomic Pt-surface holes with a pentagon almost parallel to the surface on the bridge sites of the second Pt layer. The C60 orientation (C1) is achieved by rotating the molecule by approximately -52º with respect to the C2-orientation around a [001] axis while shifting it by 0.5 Å along [1-10] direction. On the side view of the fig. 3, the Pt-Pt bonds were removed to better visualize the C-Pt bonds. The corresponding atomic coordinates of the Pt atoms in the three outermost layers and those of the C-atoms of the C60 in the *cm* asymmetric unit cell are given in Table 1. The C60 molecules are NOT embedded into the holes and stand ~0.2 Å above the topmost Pt surface layer, close to the center of the double vacancy. The first Pt-Pt interlayer distance, 1.30 Å, is significantly shorter than the bulk distance (1.375 Å) which could be due to the presence of the additional atoms in the initial (1x2) missing row, however, this distance is much larger than for the clean surface[16] (~1.1 Å). The most stable C60 configuration (referred as C1 in fig. 2) yields 15 C-Pt bonds with lengths ranging from 2.1 to 2.6 Å with an average bond distance of 2.4 ± 0.1 Å. Four C-atoms have C-Pt bond lengths lower than 2.15 Å: two of them are linked to atoms (labeled as Pt1-1) of the partially filled row while the other two (those of the 5:6 bond) are linked to Pt atoms in bridge site of the second layer (Pt2-1) (see table 1 and Fig. 2a). These two strong bonds between C60 and Pt1-1 are compensated by the other 5 C-Pt bonds on the other side of the molecule also identified as black C-atoms in fig. 2a. The molecular stability is achieved by 15 C-Pt bonds that redistribute the molecule-substrate charge transfer via a large contact area, and the coexistence of different types of covalent bonds[18]: the different bond lengths fix the molecule on the surface by minimizing the surface stress at the interface. This fact is supported by the atomic shifts off the "ideal" bulk positions of the Pt atoms at the reconstructed surface, as observed in Table 1. The effect of this strong bonding shows up as an apparent ~6% reduction of the C60 diameter, as obtained from the refinement procedure. This behavior has already been observed[19] by scanning tunneling microscopy (STM).

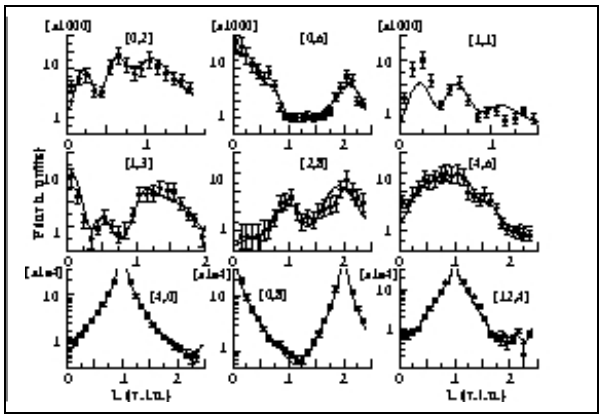

Fig. 4: Fractional and Crytal Truncational rods of the C60/Pt(110)-c(2x2) structure. The continuous lines correspond to the calculated data form the structure shown in Fig. 3.

Our STM images[10] and X-Ray diffraction results shed new light on the C60 interaction with the Pt(110) surface. Indeed, while we conclude to similar – albeit not identical – configuration for the C60 orientation with respect to the surface, the outcome of the diffraction analysis is quite at ode with density functional theory (DFT) predictions. The models taken in consideration by the DFT calculations[20] are the following: (1) c(4x4)-C60 on (1x2)-Pt, (2) chemisorbed C60 on bi- and tri-atomic vacancies on (1x1)-Pt(110) and (3) C60 adsorbed on (1x1)-Pt

without vacancies. The correct determination of both Pt atoms arrangement and C60 molecular orientation could not be achieved by DFT for the c(4x4) phase due to the wrong choice of the starting models to explain the STM images. The total energy of the system (molecules + substrate) depends on the correct choice of the vacancies distribution on Pt surface, atomic relaxations and on molecular orientation. While in the calculations, the relaxations are properly taken into account by considering an adequate number of Pt layers, DFT leads to unreliable results due to the wrong interface structure. Moreover, the DFT surprisingly prefers model (3), as the one which best agrees with STM images, instead of models (1) and (2) that described the correct c(4x4)-C60 arrangement and the correct double vacancies on Pt, respectively.

On Pd(110), C60 is supposed to adsorb on vacancies formed by Pd atoms released out of the first or the two first layers[5,6]. Regarding the molecular orientation, the adsorption on Pd and Pt presents a great similarity. Indeed, in both cases, the C60 stick to the surface through or close to a 5:6 bond. In addition, nanoholes formation is also observed on Au(110) upon C60 adsorption[21]. Since Pt has a lattice parameter between those of Au and Pd, one could reasonably expect a similar type of C60 induced vacancies on Pt than those already observed on fcc(110) metals as demonstrated from our X-ray diffraction analysis. The present results – bi-atomic vacancy model – have the advantage to give a coherent overall scheme for the fullerene-substrate configuration on large lattice constant fcc metals. A clear outcome of the 2-fold vacancy formation is that it allows maximum coordination as compared to the (1x2) case or any other substrate configuration with less dense surface layers or local environments. In this respect, the formation of nanoholes is also much more favorable than a flat layer that might occur in case of dominant molecule-molecule interaction and weak adsorbate-substrate interaction yielding a perfect hcp fullerene layer (never observed).

In conclusion, the structural properties of c(4x4)-C60/Pt(110) system have been studied by grazing incidence X-ray diffraction. The atomic arrangement at the interface of the topmost substrate atoms has been determined as well as the optimum C60 configuration. The interaction between the topmost Pt surface atoms with the fullerene molecules induces a distribution of nanoholes used as 2D template to host the quasi-hexagonally packed C60 molecules. The molecules induce a Pt surface de-reconstruction of the (1x2) missing rows that are 50% re-filled with Pt atoms. The large distribution of C-Pt bond lengths, between 2.1 and close to 2.6 Å, indicates delocalization of the charge from the molecule to the substrate among a rather large contact interface area. The interaction between C60 molecules with the topmost Pt surface layers results in a less stressed interface structure when the *cm* C60-orientation (C1 configuration) is considered. The molecule is laterally shifted by the 0.5 Å along [1-10] direction with one of its pentagon rings almost parallel to the surface on Pt bridge sites.

Element	**X ± 0.001**	**Y ± 0.001**	**Z ± 0.004**
Pt_{1-1}	0.375 + 0.024	0.000*	0.000 – 0.033
Pt_{1-2}	0.125 + 0.014	0.500*	0.000 + 0.012
Pt_{1-3}	0.125 + 0.012	0.250 + 0.012	0.000 - 0.029
Pt_{1-4}	0.375 + 0.012	0.250 + 0.007	0.000 – 0.046
Pt_{2-1}	0.000 + 0.001	0.125 + 0.000	-0.500 – 0.029
Pt_{2-2}	0.000 + 0.014	0.375 + 0.002	-0.500 + 0.020
Pt_{2-3}	0.250 + 0.005	0.125 – 0.002	-0.500 + 0.002
Pt_{2-4}	0.250 + 0.014	0.375 + 0.010	-0.500 + 0.012
Pt_{3-1}	0.125 + 0.007	0.000*	-1.000 + 0.003
Pt_{3-2}	0.375 + 0.010	0.000*	-1.000 + 0.053
Pt_{3-3}	0.125 + 0.003	0.500*	-1.000 - 0.023
Pt_{3-4}	0.375 + 0.004	0.500*	-1.000 – 0.025
Pt_{3-5}	0.125 + 0.019	0.250 – 0.000	-1.000 - 0.010
Pt_{3-6}	0.375 + 0.019	0.250 + 0.001	-1.000 + 0.013

Tab. 1: Atomic coordinates (in normalized lattice units) of atoms included in the *cm* asymmetric unit cell for the best bridge C1 model. Only the 3 topmost Pt surface layers are included. Pt_{i-j} indicates Pt atom j located in layer i.

Acknowledgements

X. T. thanks the Spanish MICINN agency for partially funding this project through project CSD2007-0004. V.L. acknowledges the support of "generalitat de Catalunya" through the 2009 SGR 1292 project and of the MEI through the MAT2007-66309-C02-02 project.

References

1. V. Langlais, X. Torrelles, Y. Gauthier & M. De Santis, Phys. Rev. B **76**, 035433 (2007)
2. M. Hinterstein, X. Torrelles, R. Felici, J. Rius, M. Huang, S. Fabris, H. Fuess and M. Pedio, Phys. Rev. B (2008)
3. Pedio-2000
4. R. Felici, M. Pedio & F. Borgatti, Nature Materials **4**, 688 (2005)
5. J. Weckesser, C. Cepek, R. Fasel, J.V. Barth, F. Baumberger, T. Greber & K. Kern, J. of Chem. Phys. 115, 19, 9001-9009 (2001)
6. J. Weckesser, J.V. Barth, & K. Kern, Phys.Rev. B 64, 19, 161403 (2001)
7. T. David, J.K. Gimzewski,D. Purdie, B. Reihl, R. Schlittler, Phys. Rev. B 50 5810-5813 (1994)
8. H. I. Li, K. Pussi, K. J. Hanna, L.-L. Wang, D. D. Johnson, H.-P. Cheng, H. Shin, S. Curtarolo, W. Moritz, J. A. Smerdon, R. McGrath, and R. D. Diehl, Phys. Rev. Lett. **103**, 056101 (2009)
9. M. Hinterstein, X. Torrelles, R. Felici, J. Rius, M. Huang, S. Fabris, H. Fuess, and M. Pedio, Phys. Rev. B **77**, 153412 (2008)
10. Langlais *et al*. in preparation (2009)
11. R. Baudoing-Savois, G. Renaud, M. de Santis, A. Barbier, O. Robach, P. Taunier, P. Jeantet, O. Ulrich, J. P. Roux, M. C. Saint-Lager, A. Barski, O. Geaymont, G. Berard, P. Dolle, M. Noblet & A. Mougin, Nuc. Instru. Methods Phys. Res. B 149, 213 (1999)
12. R. Feidenhans'l, Surface Science Reports **10**, 105 (1989)
13. I. K. Robinson, *Handbook of Synchrotron Radiation*, vol. 3 (North Holland Amsterdam, 1991)
14. E. Vlieg, J. Appl. Crystallogr. 33, 401 (2000).
15. Thermal vibrations parameters were assumed identical for all C atoms of the molecule (B_C = 14 Å^2). Meanwhile, different values were assigned to Pt atoms to both types of rows in the top layer: $B_{Pt\text{-}top\text{-}part}$ = 9 Å^2 (partially filled missing row) and $B_{Pt\text{-}top\text{-}filled}$ = 6 Å^2 (filled row). Deeper layers were given the following values: $B_{Pt\text{-}2}$ = 2 Å^2, $B_{Pt\text{-}3}$ = 0.7 Å^2, $B_{Pt\text{-}4}$ = 0.3 Å^2 and $B_{Pt\text{-}5}$ = 0.3 Å^2. The root mean square vibration amplitude (u, $B = 8\pi^2\langle u^2\rangle$), is 0.4 Å for C atoms and 0.2 Å for the (averaged) top layer. Moreover, right thermal vibrations contribute to a reduction by almost 2 of the agreement factor and a significant further decrease is obtained with optimum Pt parameters.
16. P. Fery, W. Moritz & D. Wolf, Phys. Rev. B 38, 7275 (1988).
17. M. Casarin, D. Forrer, T. Orzali, M. Petukhov, M. Sambi, E. Tondello & A. Vittadini, J. Phys. Chem. C 111, 9365 (2007)
18. C. Cepek. A. Goldoni & S. Modesti, Phys. Rev. B 53, 7466 (1996)
19. T. Orzali, M. Petukhov, M. Sambi & E. Tondello, Appl. Surf. Sci. 252, 5534, (2006)
20. T. Orzali, D. Forrer, M. Sambi, A. Vittadini, M. Casarin & E. Tondello, J. Phys. Chem. C 112, 378 (2008)
21. M. Hinterstein, X. Torrelles, R. Felici, J. Rius, M. Huang, S. Fabris, H. Fuess, and M. Pedio, Phys. Rev. B 77, 153412 (2008)